Advances in Engineering Research : Possibilities and Challenges
ISSN Print: 3079-5192
ISSN Online: 3079-5206
https://doi.org/10.63313/AERpc.9050

Tribological properties of CF/PEEK paired with different metals

Hongqian Ma[1]. Youqiang Wang[1.2]
[1]Qingdao University of Technology, School of Mechanical and Automotive Engineering, Qingdao 266520, China
[2]Qingdao University of Technology, Key Lab of Industrial Fluid Energy Conservation and Pollution Control, Qingdao 266520, China

How to cite this paper: Ma, H. Q., & Wang, Y. Q. (2025). Tribological properties of CF/PEEK paired with different metals. Advances in Engineering Research : Possibilities and Challenges, 2(2), 67-80. ISSN Print: 3079-5192; ISSN Online: 3079-5206.
https://doi.org/10.63313/AERpc.9050
Published: 2025-08-29

Abstract

Under the condition of impurity water lubrication, the tribological properties of three friction pairs consisting of 45#, nickel-plated steel, 304L, and carbon fiber-reinforced PEEK composite (CF/PEEK) were investigated. Ball-on-block reciprocating tests were conducted using a self-made friction and wear tester. In combination with surface morphology characterization, the friction and wear mechanisms of the materials were deeply analyzed. The research results showed that with changes in load and rotational speed, the friction coefficient and wear volume of CF/PEEK-45# were consistently lower than those of CF/PEEK-NP and CF/PEEK-304L. Under the condition of impurity water lubrication, the compatibility of CF/PEEK with the three materials was ranked as follows: CF/PEEK-45# > CF/PEEK-NP > CF/PEEK-304L. This study provides key data support and theoretical guidance for the practical application of CF/PEEK composite materials in motion pair components such as water-lubricated bearings and guide rails.

Keywords

CF/PEEK; 45# steel; water lubrication with impurities; friction pair; friction and wear

1. Introduction

With the global deepening implementation of the "Carbon Peak and Carbon Neutrality" strategy, coupled with continuously growing energy demand and increasing pressure from fuel costs, energy conservation and emissions reduction have become both a societal consensus and an urgent task[1]. Particularly in waterborne operating equipment, the severe threat posed by traditional lubricant leakage to marine and river environments has driven a shift towards more environmentally friendly solutions. As a green and clean lubrication technology, water-lubricated bearings have been widely adopted in fields such as ship propulsion systems, turbines, hydroelectric power plants, and pumps. In the context of today’s green development, the performance requirements for water-lubricated bearings are also increasing, especially in terms of lubrication and friction, vibration damping, and noise reduction. To meet these demands, the selection and use of green, high-performance materials have become crucial[2][3]. From traditional metals to later developments like Thordon, and now further research and improvement of polymer materials[4], the choice of materials in this field has been continuously evolving.

Compared to commonly used metals and ceramics, polymer materials offer advantages such as corrosion resistance, excellent self-lubrication capability, and lightweight properties, making them widely applicable in automotive, medical devices, aerospace, and electronic equipment fields[5-8]. There are many types of polymers, among which polyetheretherketone (PEEK) is a typical polymer material and has been extensively used[9-12]. In comparison to traditional polymer materials, PEEK exhibits excellent heat resistance, radiation resistance, corrosion resistance, impact resistance, and flame retardancy. Research on PEEK, both domestically and internationally, tends to focus more on its tribological properties under dry friction[13] and water-lubricated conditions when compounded with other materials or used as a modifying agent. Currently, filler modification methods for PEEK include reinforcement with inorganic fillers (such as polytetrafluoroethylene, graphite, molybdenum disulfide, carbon nanotubes, etc.), inorganic particle reinforcement (e.g., SiC, SiN, Al_2O_3, $CaCO_3$, ZrO_2, SiO_2, etc.), fiber reinforcement (including glass fiber GF and carbon fiber CF), and polymer blending modification. Literature [14] investigated PEEK/graphite composites with excellent tribological properties. The friction coefficient of PEEK/graphite composites was found to be lower than that of pure PEEK. Literature [15] and [16] studied the tribological properties of nano-SiC and nano-SiN filled PEEK materials, respectively. The results showed that, compared to pure PEEK, nano-SiC and SiN significantly reduced the friction coefficient and wear rate. Literature [17] prepared PEEK/PTFE composites with low friction and ultra-low wear properties, investigating the effect of PTFE addition on the tribological performance of PEEK. The results indicated that after adding PTFE to PEEK, the friction coefficient of PEEK/PTFE was further reduced.

Currently, the use of PEEK as a material for lubricated bearings has been reported in the literature [18-20]. Researchers worldwide have shown a greater inclination toward studying the tribological properties of PEEK when blended with other materials or used as an additive under various lubrication conditions. Literature [21] systematically investigated the tribological performance of PEEK and its composites—GF/PEEK, CF/PEEK, and PTFE/PEEK—paired with GCr-15 under three lubrication conditions (dry friction, oil lubrication, and starved lubrication). The study found that under all lubrication states, the addition of CF, GF, and PTFE improved the tribological properties of PEEK-based materials, with CF/PEEK exhibiting the most outstanding performance. Literature [22] examined the tribological characteristics of CF/PEEK-Si_3N_4 pairs under water-lubricated conditions. The results indicated that the friction coefficient of CF/PEEK-Si_3N_4 composites in water lubrication was significantly lower than that under dry friction conditions. Sliding speed had a more pronounced effect on the friction coefficient than pressure, and an increase in speed led to a reduction in the friction coefficient. Literature [23] compared the wear and friction properties of PEEK, PEEK-CF30, and PEEK-GF30 against carbon steel AISI 1045 under dry friction conditions. The results showed that PEEK-CF30 had the lowest friction coefficient, followed by PEEK, while PEEK-GF30 exhibited a relatively high friction coefficient throughout the sliding distance. Literature [24] explored the tribological characteristics of three stainless steel (AISI 316L, AISI 630, and S32750)/PEEK friction pairs in a seawater environment. The study revealed that the average friction coefficients of the three pairs were nearly identical; under heavy load conditions, S32750/PEEK demonstrated the best frictional stability, while AISI 316L/PEEK showed the poorest.Although extensive research has been conducted on the friction and wear properties of PEEK composites by scholars worldwide, most studies have focused on their tribological performance in simple environments. Considering the economic applicability of different friction pair materials and the need to expand their application scope, the authors of this paper employed a ball-on-disk reciprocating contact configuration and a controlled-variable approach to investigate the tribological performance of CF/PEEK paired with three different counter balls under impurity-laden water lubrication (94.3% deionized water + 3.5% NaCl + 1% peanut oil + 1.2% SiO_2). The aim is to identify the most compatible counter material for CF/PEEK.

2. Experimental Section

2.1. Test equipment and parameters

The lower specimens used in this study were made of PEEK supplied by Dongguan Xinyao Plastic Products Co., Ltd., with uniform geometrical dimensions of 30 mm × 20 mm × 5 mm and a surface roughness (Ra) ranging between 0.2 μm and 0.25 μm. The upper specimens consisted of 45# steel balls (Ra: 0.020–0.030 μm, diameter: 9.525 mm), nickel-plated steel balls (electroplated Q235 steel, denoted as NP) (Ra: 0.020–0.030 μm, diameter: 9.525 mm), and 304L stainless steel balls (Ra: 0.020–0.030 μm, diameter: 9.525 mm).

2.2. Test method and related characterization

This study employed a controlled-variable experimental approach to systematically investigate the tribological performance of CF/PEEK paired with three different materials under impurity-laden water lubrication conditions. The test parameters were set with reference to the actual working conditions of garbage truck compression loading mechanisms and typical testing conditions for water-lubricated bearings: rotational speeds were set at 60, 80, 100, and 120 r/min (corresponding to linear velocities of 20.0, 26.7, 33.3, and 40.0 mm/s), loads at 35 N, 50 N, 65 N, and 80 N, and a fixed sliding time of 30 min (ensuring the friction and wear process reached a stable state), with a single-pass wear scar length of 10 mm. Friction coefficient-time curves were recorded, and at least three repeated tests were conducted to calculate the average friction coefficient and wear rate. All experimental data were recorded online at a sampling rate of 80 Hz using a self-programmed LabVIEW (National Instruments) program. The test was designed with a lubricant emulsion containing 3.5% NaCl, 1% peanut oil, and 1.2% silt (94.3% deionized water + 3.5% NaCl + 1% peanut oil + 1.2% SiO_2). This lubrication condition was designed to simulate both the actual working conditions that garbage truck guide rail systems may face, such as contamination from food waste and intrusion of particulate impurities, as well as, to some extent, the harsh operating environments of marine water-lubricated bearings, such as silt-laden seawater and oil leakage.

Before and after the tests, the CF/PEEK specimens and friction surfaces were cleaned with anhydrous ethanol and dried. A high-precision electronic balance (accuracy: 1×10^{-4} g) was used to weigh the CF/PEEK specimens, and the wear loss was determined by calculating the mass difference before and after the tests. To reveal the tribological performance of PEEK, the worn surfaces of the samples were analyzed using a scanning electron microscope (Sigma 300 model).

2.3. Control variable experimental design

Two sets of controlled-variable experiments were conducted: The first set maintained a constant rotational speed of 100 r/min to evaluate the tribological properties of three friction pairs under loads of 35 N, 50 N, 65 N, and 80 N. The second set maintained a constant load of 50 N to analyze the tribological characteristics of the three friction pairs at rotational speeds of 60 r/min, 80 r/min, 100 r/min, and 120 r/min.

3. Analysis of friction and wear test

3.1. The influence of load variation on the tribological performance of different friction pairs

3.1.1. The influence of load on the friction coefficient of CF/PEEK

Figure 1 shows the friction coefficients of CF/PEEK against three different counter materials under impurity-laden water lubrication, at a fixed rotational speed of 100 r/min and varying loads. According to friction theory[25], the friction and wear of materials can be divided into three stages: running-in wear, stable wear, and severe wear. Based on the experimental data and observed friction coefficients, it is concluded that no severe wear stage occurred. As seen in Figure 1(a) to 1(c), the friction process can be divided into two typical stages: the initial running-in stage, during which the friction coefficient gradually increases over time, followed by a stable stage, where fluctuations diminish and the value eventually stabilizes. The results indicate that the friction coefficient ranges for CF/PEEK-45# steel, CF/PEEK-NP, and CF/PEEK-304L were 0.11949–0.14318, 0.1584–0.19169, and 0.16294–0.19964, respectively. CF/PEEK-45# exhibited the lowest friction coefficient, while the values for CF/PEEK-NP and CF/PEEK-304L were very similar. As the load increased from 35 N to 80 N, the average friction coefficients of both CF/PEEK-NP and CF/PEEK-304L showed a consistent trend: an initial increase followed by a decrease. The primary reason for this behavior is that, despite the presence of a water film, its lubricating effectiveness gradually diminishes with increasing load. Higher loads lead to an increase in the real contact area between the friction pairs, making it easier for hard asperities such as carbon fibers (CF) in the composite to penetrate and disrupt the boundary water lubrication film. This enhances direct contact and plowing effects at the interface, resulting in an increase in the friction coefficient. However, when the load exceeded 50 N, the friction coefficient began to decrease, which can be attributed to a significant enhancement in tribochemical effects. The combined action of extreme contact pressure and frictional heat promotes complex chemical reactions among water molecules, NaCl, SiO_2, the PEEK composite, and the metal surface, forming a self-lubricating reaction film. In contrast, the average friction coefficient of CF/PEEK-45# decreased linearly from 0.12829 to 0.11949 as the load increased. This is primarily due to a transition in the contact state at the friction interface and the effectiveness of the lubrication film. Specifically, at lower loads, the friction pair operates under boundary lubrication conditions with considerable asperity contact, resulting in mild abrasive wear and a relatively higher friction coefficient. As the load increases, significant elastic deformation occurs in CF/PEEK, which facilitates the formation of a more stable hydrodynamic lubrication film, effectively reducing the friction coefficient. This process is accompanied by an increased contact area that allows for better access to lubricating media, promoting the formation of a continuous water film that effectively separates the contacting surfaces and significantly improves tribological performance. Therefore, the tribological properties of CF/PEEK-45# are enhanced under heavy loads.

In Figure 1(d), the friction coefficient of CF/PEEK-304L is higher than those of CF/PEEK-45# and CF/PEEK-NP, reflecting its inferior frictional stability. Compared to CF/PEEK-45# and CF/PEEK-NP, CF/PEEK-304L exhibits more pronounced vibrations due to its higher metal hardness and strength. Additionally, it can be observed that the friction coefficient of CF/PEEK-304L is slightly higher than that of CF/PEEK-NP. In summary, when paired with CF/PEEK, the three stainless steel materials exhibit frictional stability in the following descending order: CF/PEEK-45# > CF/PEEK-NP > CF/PEEK-304L.

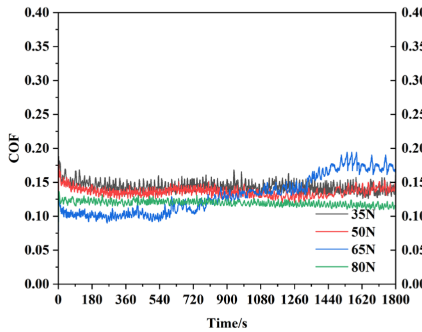

（a）CF/PEEK-45#

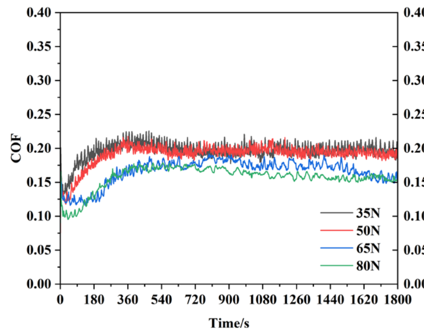

（b）CF/PEEK-NP

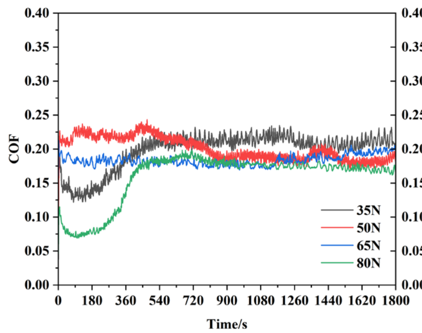

（c）CF/PEEK-304L

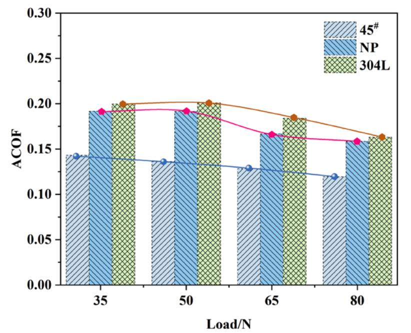

（d）Average coefficient of friction

Figure 1. Frictional traces under different applied loads

3.1.2. Effect of Load on the Wear Rate of CF/PEEK

Figure 2 shows the wear loss of CF/PEEK-45#, CF/PEEK-NP, and CF/PEEK-304L under different loads. As can be seen from the figure, the wear loss of CF/PEEK-NP and CF/PEEK-304L is relatively similar, while CF/PEEK-45# exhibits the lowest wear loss. When the load increases from 35 N to 80 N, the wear loss of CF/PEEK-45#, CF/PEEK-NP, and CF/PEEK-304L consistently decreases, albeit to a minor extent. This indicates that the wear loss of these three material pairs is relatively insensitive to changes in load. The primary reasons for this behavior are as follows: First, as the load increases, the lubrication film between the friction pairs is compressed and ruptured, causing SiO_2 particles to become embedded in the surface of the softer material or form a third-body layer, which subsequently acts to reduce friction. Second, the increased load may promote tribochemical reactions, accelerating the adsorption of corrosion products from the NaCl solution or decomposition products of the edible oil, thereby forming a boundary lubrication film. Additionally, the passive films on 304L and NP may become more stable under high stress, while the plastic deformation of 45# steel enhances surface work-hardening effects. These factors collectively contribute to an anomalous decrease in wear loss within specific load ranges.Furthermore, CF/PEEK can form a transfer film on the friction surface during the sliding process. Within a certain range, as the load increases, the transfer film becomes more continuous and complete, thereby reducing wear loss.

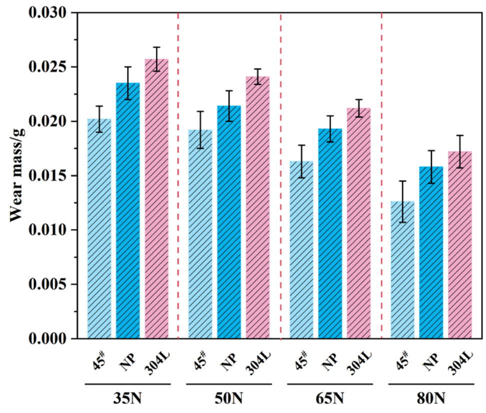

Figure 2. The wear mass of different friction pair combinations for PEEK and CF/PEEK composite materials under varying loads

3.1.3. Effect of Load on the Worn Morphology of CF/PEEK

Since the differences in the worn surfaces of the three friction pairs were most pronounced at a load of 65 N, the disk specimens of the three pairs were examined at this load. Figure 3 shows the worn surfaces of CF/PEEK observed via SEM after tribological tests under impurity-laden water lubrication. Comparing Figure 3(a)–3(c), it can be seen that under light loading, the worn surface of the 45# pair is smoother and more uniform than those of NP and 304L, which corresponds to the lower friction coefficient observed for CF/PEEK-45#. As shown in Figure 3(a), at a load of 65 N, the worn surface of CF/PEEK exhibits fine wear debris particles and shallow scratches. The primary wear mechanism is abrasive wear, accompanied by mild adhesive wear and corrosive wear in a mixed mode. Hard particles such as SiO_2 are embedded into or slide across the relatively soft PEEK matrix under load, causing micro-cutting and forming shallow ploughing grooves. Meanwhile, cyclic loading and mechanical action lead to carbon fiber (CF) breakage or debonding from the matrix, generating fine debris. The presence of NaCl solution induces mild electrochemical corrosion, weakening the surface strength and accelerating wear. Although the mixture of trace edible oil and water provides partial lubrication and reduces direct metal contact, it fails to form a complete and effective lubricating film, resulting in localized adhesion and material transfer. As shown in Figure 3(b), the worn surface displays a small amount of debris and distinct ploughing grooves parallel to the sliding direction. The wear mechanism is characterized by mild abrasive wear accompanied by ploughing. This indicates that hard particles such as SiO_2 or exposed CF reinforcements in the composite cause micro-cutting and plastic deformation on the NP surface. Although the impurity-laden water lubrication film partially mitigates adhesive wear, it cannot fully prevent the mechanical action of abrasive particles, ultimately leading to micro-ploughing and material removal. Figure 3(c) reveals mild abrasive wear and severe adhesive wear. Despite the presence of lubricating media such as water and edible oil, the combination of relatively low load (65 N) and rotational speed (100 r/min) is insufficient to generate adequate hydrodynamic effects for forming a complete lubricating film. This results in frequent direct contact between the PEEK matrix of the CF/PEEK composite and the 304L surface. Localized high temperatures and pressures soften or even melt the PEEK material, causing strong adhesion to the metal surface. Subsequent relative sliding leads to tearing and material transfer, resulting in severe adhesive wear. Simultaneously, hard particles like SiO_2 and detached CF fragments in the lubricant are pressed into the softened PEEK surface under load, causing micro-cutting and ploughing, thereby inducing mild abrasive wear.

（a）CF/PEEK-45# （b）CF/PEEK-NP （c）CF/PEEK-304L

Figure 3. Wear surface morphology of CF/PEEK composite material

3.2. Effect of Rotational Speed on the Tribological Properties of Different Friction Pairs

3.2.1. Effect of Rotational Speed on the Friction Coefficient of CF/PEEK

Figure shows the friction coefficients of CF/PEEK paired with three types of steel under impurity-laden water lubrication as a function of rotational speed. It can be observed that the average friction coefficients of all three pairs were initially relatively high. As the rotational speed increased from 60 r/min to 100 r/min, distinct trends emerged: the average friction coefficient of CF/PEEK-45# gradually increased to 0.13616, while CF/PEEK-304L and CF/PEEK-NP exhibited a similar trend, initially decreasing and then increasing. When the rotational speed further increased to 120 r/min, the average friction coefficient of CF/PEEK-45# decreased rapidly to 0.11287, whereas the friction coefficients of CF/PEEK-304L and CF/PEEK-NP declined to approximately 0.14812, stabilizing at a similar level.

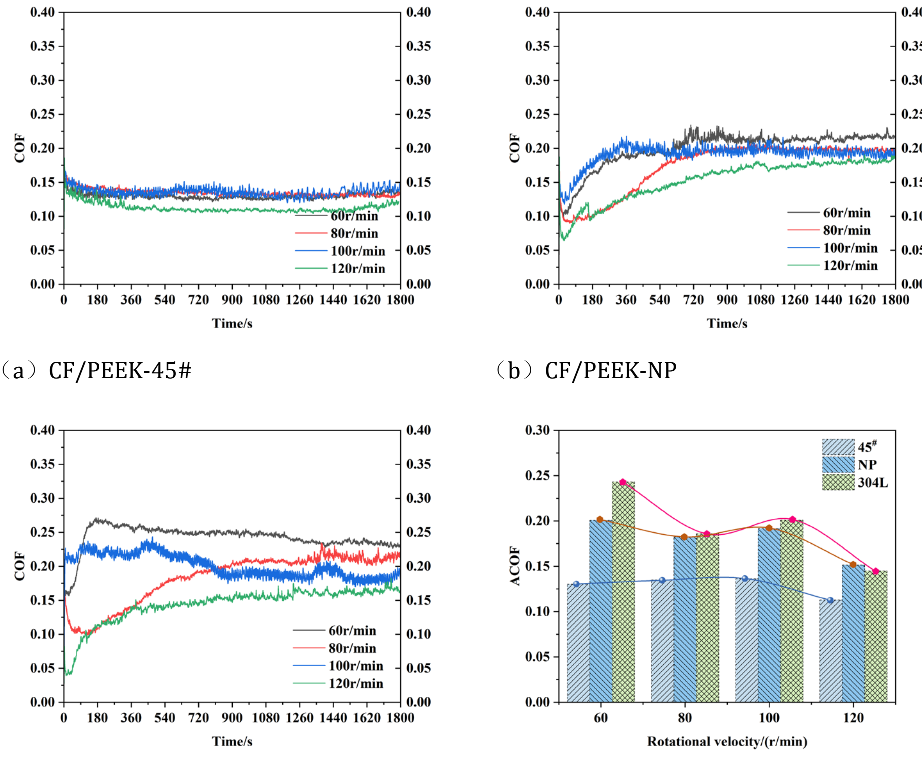

（a）CF/PEEK-45#

（b）CF/PEEK-NP

（c）CF/PEEK-304L

（d）Average coefficient of friction

Figure 4. Fictional traces under different rotational velocities

Under impurity-laden water lubrication, the average friction coefficient of CF/PEEK-45# exhibits a nonmonotonic trend with increasing rotational speed, attributed to transitions in the dominant friction mechanisms across different speed ranges. As the rotational speed increases from 60 r/min to 100 r/min, the friction coefficient rises due to insufficient hydrodynamic effects in this speed range. The increased sliding frequency accelerates the plowing action of SiO_2 abrasive particles and the cutting effect of carbon fibers (CF) on the surface, making abrasive wear the dominant mechanism. When the speed further increases to 120 r/min, the enhanced rotational velocity promotes more efficient entry of lubricating media into the contact zone, strengthening the hydrodynamic effect. Simultaneously, frictional heat induces local softening of the PEEK surface, forming a lubricating transfer film that improves the lubrication state, thereby significantly reducing the friction coefficient. For CF/PEEK-304L and CF/PEEK-NP pairs, the average friction coefficient under impurity-laden water lubrication first decreases, then increases, and finally decreases again as the rotational speed increases from 60 r/min to 120 r/min, eventually stabilizing at approximately 0.14812. Initially, at 80 r/min, the enhanced hydrodynamic effect facilitates the formation of a thicker lubricating film, reducing the friction coefficient. When the speed increases to 100 r/min, the higher sliding frequency and shear rate intensify the grinding action of hard particles such as SiO_2, compromising the integrity of the lubricating film and causing the friction coefficient to rebound. As the speed further rises to 120 r/min, the 显著 increase in frictional heat induces local softening and even melting of the PEEK surface, generating a lubricating transfer film. Additionally, elevated temperatures may alter the viscosity and lubricating properties of the impurity-laden solution, contributing to a renewed reduction in the friction coefficient. Ultimately, the friction coefficient stabilizes when a dynamic balance is achieved among lubricating film formation, disruption, and thermal effects.

Compared to NP and 304L, 45# steel likely possesses superior corrosion resistance and smoother surface characteristics, enabling better synergy with CF/PEEK. This results in reduced susceptibility to lubricating film rupture at high speeds, thereby demonstrating consistently superior tribological performance.

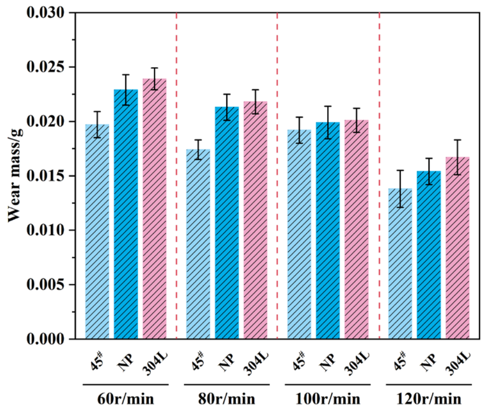

Figure 5. The wear mass of different friction pair combinations for PEEK and CF/PEEK composite materials under varying rotational velocities

3.2.2. Effect of Rotational Speed on the Wear Loss of CF/PEEK

Figure 5 shows the wear loss of CF/PEEK-45#, CF/PEEK-NP, and CF/PEEK-304L under different rotational speeds. The wear loss of NP and 304L pairs remains relatively similar, while that of 45# is consistently the lowest. As the rotational speed increases from 60 r/min to 120 r/min, the wear loss of all three material pairs gradually decreases. This indicates that the wear loss of CF/PEEK-45#, CF/PEEK-NP, and CF/PEEK-304L is only marginally influenced by rotational speed. CF/PEEK exhibits excellent mechanical properties and wear resistance, with its wear behavior primarily governed by the microscopic mechanical interactions between the hard carbon fiber (CF) reinforcements and the counter steel surface, as well as the potential formation of thin transfer films. Although increased rotational speed introduces more lubricating medium into the contact zone, improving frictional heat dissipation and surface lubrication conditions, the limited lubricating performance of the impurity-laden water prevents the formation of a sufficiently thick and stable hydrodynamic lubricating film capable of altering the fundamental wear mechanisms at the interface. Therefore, the slight reduction in wear loss can be attributed to enhanced cooling effects and more efficient expulsion of abrasive particles at higher speeds, which mitigate adhesion and corrosion tendencies. However, the dominant wear mechanism remains abrasive wear caused by CF, resulting in no significant change in overall wear loss. Additionally, the highest hardness of 45# steel provides optimal support, effectively suppressing abrasive particle embedding and plastic deformation, which explains its consistently lowest wear loss across all tested speeds.

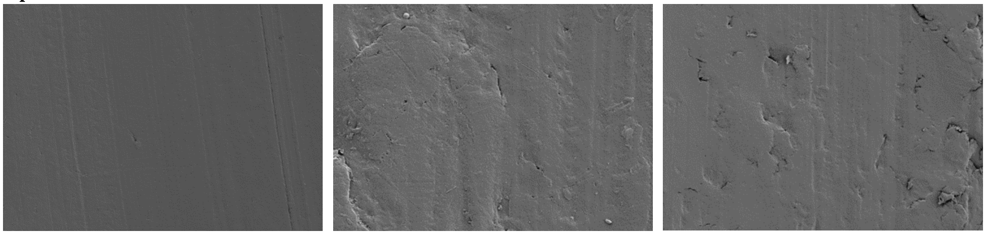

（a）CF/PEEK-45# （b）CF/PEEK-NP （c）CF/PEEK-304L

Figure 6. Wear surface morphology of CF/PEEK composite materia

3.2.3. Effect of Rotational Speed on the Worn Surface of CF/PEEK

Since the differences in the worn surfaces of the three friction pairs were most pronounced at a rotational speed of 60 r/min, the disk specimens of the three pairs were examined at this speed. Figure 6 shows the worn surfaces of CF/PEEK observed via SEM after tribological tests under impurity-laden water lubrication.

Comparing Figures 6(a)–6(c), it can be seen that at lower rotational speeds, the worn surface of CF/PEEK-45# is smoother and more uniform than those of CF/PEEK-NP and CF/PEEK-304L. As shown in Figure 6(a), the worn surface of CF/PEEK-45# exhibits only small-area spalling pits but numerous ploughing grooves parallel to the sliding direction. The formation of parallel grooves is primarily attributed to hard SiO_2 particles in the lubricating medium and exposed hard carbon fibers (CF) in the composite, which embed into the 45# steel surface under normal load, causing micro-cutting. Meanwhile, the small spalling pits likely result from flake-like debris detachment due to fatigue or local adhesion under cyclic loading. Although the impurity-laden water provides certain lubrication and cooling effects, it fails to fully eliminate the ploughing effect caused by hard particles, resulting in a wear surface dominated by abrasive wear characteristics. Figure 6(b) shows that the worn surface of CF/PEEK-NP exhibits numerous short and shallow surface cracks. These cracks predominantly occur at the interfaces between CF and the PEEK matrix, where lower surface strength makes them prone to detachment under cyclic stress, subsequently forming cracks. The primary wear mechanism is abrasive wear. As observed in Figure 6(c), the worn surface of CF/PEEK-304L displays large-area grooves, minor spalling pits, and distinct material adhesion features. The wear mechanism is characterized by mild abrasive wear accompanied by adhesive wear. At lower rotational speeds, the temperature rise on the friction surface is limited. The hard asperities of the 45# steel surface exhibit weaker cutting effects on the softer modified PEEK surface, while partial material tearing at adhesion points leads to the formation of adhesive spalling pits.

4. Conclusion

This study systematically investigated the tribological properties of CF/PEEK composites paired with 45#, NP, and 304L under impurity-laden water lubrication. The main conclusions are as follows:

(1) Under varying loads and rotational speeds, significant differences were observed in the tribological performance of CF/PEEK paired with the three metals. Based on comprehensive friction coefficients and wear loss, the order of compatibility is: CF/PEEK-45# > CF/PEEK-NP > CF/PEEK-304L. Due to its higher hardness and excellent surface supportability, 45# steel forms the optimal friction pair with CF/PEEK, exhibiting the lowest and most stable friction coefficient and the smallest wear loss.

(2) As the load increased (35 N to 80 N), the friction coefficient of CF/PEEK-45# decreased linearly and slightly, primarily attributed to the enhanced elastohydrodynamic lubrication effect and the formation of a more stable transfer film under higher loads. In contrast, the friction coefficients of CF/PEEK-NP and CF/PEEK-304L initially increased and then decreased, peaking around 50 N. This trend is due to intensified abrasive wear at medium loads, while tribochemically generated self-lubricating films dominated the friction behavior at higher loads. The wear loss of all three pairs decreased slightly with increasing load, indicating that load is not the dominant factor influencing wear.

(3) The effect of rotational speed variations (60 r/min to 120 r/min) on the friction coefficient exhibited complex monotonic behavior. The friction coefficient of CF/PEEK-45# first increased and then decreased, reaching its maximum at 100 r/min. Meanwhile, CF/PEEK-NP and CF/PEEK-304L showed an initial decrease, followed by an increase and subsequent decrease, eventually stabilizing at approximately 0.148 at 120 r/min. These variations result from the competition and balance among hydrodynamic effects, abrasive wear, and frictional thermal effects. The cooling effect and improved expulsion efficiency of impurities at higher speeds slightly reduced the wear loss of all pairs, though the magnitude of this influence was limited.

(4) The primary wear mechanism for all three pairs was abrasive wear, accompanied by varying degrees of adhesive wear and fatigue spalling. The worn surface of CF/PEEK-45# was the smoothest, characterized by shallow ploughing grooves. CF/PEEK-NP exhibited short and shallow surface cracks, while CF/PEEK-304L showed the most severe adhesive features and large-area grooves, which are related to the surface characteristics of 304L and its poor compatibility with PEEK.

The study confirms that 45# steel is the optimal material choice for pairing with CF/PEEK. This research provides critical data support and a theoretical basis for the practical application of CF/PEEK composites in water-lubricated bearings, guide rails, and other moving components, particularly in complex impurity-laden water environments.

Acknowledgements

Funding Project: National Natural Science Foundation of China (52074161); Shandong Provincial Natural Science Foundation (ZR2021ME063); Special Fund for Mount Taishan Scholars Program (tsqn202211177).

References

[1] WANG Y C, WANG Y Q, ZHAO T, et al. Research progress on modification of water lubricated polymer bearing materials[J]. Bearing, 2023, (08): 1-8.

[2] XI X H. A review of research on engineering plastics[J]. Shandong Chemical Industry, 2024, 53 (03):84-86.

[3] LIN Y J. Research and Application of PEEK Materials[J]. Volkswagen Standardization, 2023, (17): 124-126.

[4] Li W Z, Yan N, Deng F, et al. Research Status of Friction and Wear Properties of Engineering Plastics under WaterLubrication[J]. Chemical New Materials, 2022, 50 (01): 30-33+38.

[5] WAN L, LIU L B, MA Y, etc Study on the Friction and Wear Characteristics of Silicon Carbide Ceramics and Polyether Ether Ketone Composite Materials [J]. Bearing, 2020, (05): 22-26.

[6] LI YUNKAI, WANG YOUQIANG, XIE YINONG, etc Study on the tribological properties of PA66under different lubrication conditions [J]. Journal of Trilogy, 2019,39 (06): 706-712.

[7] WANG Q H, XUE Q, SHEN W, et al. The frictionand wear properties of nanometer ZrO2 - filled Polyetheretherketone [J]. Journal of applied polymer science, 1998, 69(1): 135-141.

[8] PAN G L, GUO Q, ZHANG W, et al. Fretting wear behaviors of nanometer Al2O3 and SiO2 reinforced PEEK composites[J]. Wear, 2009, 266(11-12): 1208-1215.

[9] LIU H, SU X, TAO J, et al. Effect of SiO2 nanoparticles-decorated SCF on mechanical and tribological properties of cenosphere/SCF/PEEK composites[J]. Journal of Applied Polymer Science, 2020, 137(22): 48749.

[10] SHANG Y S, ZHAO Y, LIU Y, et al. The effect of micron-graphite particle size on the mechanicaland tribological properties of PEEK Composites[J]. High Performance Polymers, 2018, 30(2): 153-160.

[11] PUÉRTOLAS J A, CASTRO M, MORRIS J A, etal. Tribological and mechanical properties of graphene nanoplatelet/PEEK composites[J]. Carbon, 2019,141: 107-122.

[12] HOU X, BAI P, LI J, et al. MoS2 reinforced PEEK composite for improved aqueous boundary lubrication[J]. Friction, 2023, 11(9): 1660-1672.

[13] LI CHAOFENG. Preparation and Triboelectric Properties of PEEK based Lubrication Reinforced Composite Materials [D]. Northeastern University, 2019.

[14] SHANG Y S, ZHAO Y, LIU Y, et al. The effect of micron-graphite particle size on the mechanicaland tribological properties of PEEK Composites[J].High Performance Polymers, 2018, 30(2): 153-160.

[15] Wang Q H, Xu J, Shen W, et al. The effect of nanometer SiC filler on the tribological behavior of PEEK[J]. Wear, 1997, 209(1-2): 316-321.

[16] Wang Q H, Xu J, Shen W, et al. An investigationof the friction and wear properties of nanometer Si3N4 filled PEEK[J]. Wear, 1996, 196(1-2): 82-86.

[17] DAVID L B BURRIS D L, SAWYER W G. A low frictionand ultra low wear rate PEEK/PTFE composite[J]. Wear, 2006, 261(3-4): 410-418.

[18] HUFENBACH W, KUNZE K, BIJWE J. Sliding wear behaviour of PEEK - PTFE blends[J]. Journal of synthetic lubrication, 2003, 20(3): 227-240.

[19] QU S R, PENARANDA J, WANG S S. Tribological behavior of PTFE/PEEK composite[C]// Technical Conference. 2016.

[20] XIONG D S, LIU L L. Preparation and tribological properties of Polyetheretherketone composites[J].Journal of Biomedical Materials Research Part B:Applied Biomaterials, 2010, 93(2): 492-496.

[21] CHEN B, WANG J, YAN F. Comparative investigation on the tribological behaviors of CF/PEEK composites under sea water lubrication[J]. Tribology International, 2012, 52: 170-177.

[22] TANG Q, CHEN J, LIU L. Tribological behaviours of carbon fibre reinforced PEEK sliding on silicon nitride lubricated with water[J]. Wear, 2010, 269(7-8): 541-546.

[23] DAVIM J P, CARDOSO R. Effect of the reinforcement (carbon or glass fibres) on friction and wearbehaviour of the PEEK against steel surface at long dry sliding[J]. Wear, 2009, 266(7-8): 795-799.

[24] ZHANG Z H, NIE S L, ZHANG Z A, et al. Comparison of Tribological Characteristics of Different Stainless Steels under Seawater Lubrication [J]. Machine Tool & Hydraulics, 2019, 47(07): 1-5.

[25] Gou R, Luo X, Chen J, et al. Study on the tribological properties of diamond and SiC interactions using atomic scale numerical simulations[J]. Tribology International, 2023, 178: 108093.